Journal of Hazardous Materials 505 (2026) 141421

Contents lists available at ScienceDirect

Journal of Hazardous Materials

journal homepage: www.elsevier.com/locate/jhazmat

Synergistic enhancement of copper recovery from recalcitrant mineral phases by plant microbial fuel cells

Hang Qian [a,*], Zhenghui Gao [b], Devin Sapsford [a], Wenli Chen [c], Qiaoyun Huang [c,d,**], Michael Harbottle [a,*]

[a] School of Engineering, Cardiff University, Cardiff CF24 3AA, UK
[b] Key Lab of Urban Environment and Health, Institute of Urban Environment, Chinese Academy of Sciences, Xiamen 361021, PR China
[c] National Key Laboratory of Agricultural Microbiology, Huazhong Agricultural University, Wuhan 430070, PR China
[d] Hubei Key Laboratory of Soil Environment and Pollution Remediation, Huazhong Agricultural University, Wuhan 430070, PR China

HIGHLIGHTS

- PMFCs synergistically mobilised and recovered Cu from recalcitrant malachite.
- PMFC-driven Cu recovery reached 6.68 % in 2 months, 1.80 × higher than plant-only.
- PMFCs raised water-layer Cu to 2.89 mg/L, 36 × higher than electrokinetic-only.
- Root exudates plus circuit-driven ion transport increased Cu availability.

GRAPHICAL ABSTRACT

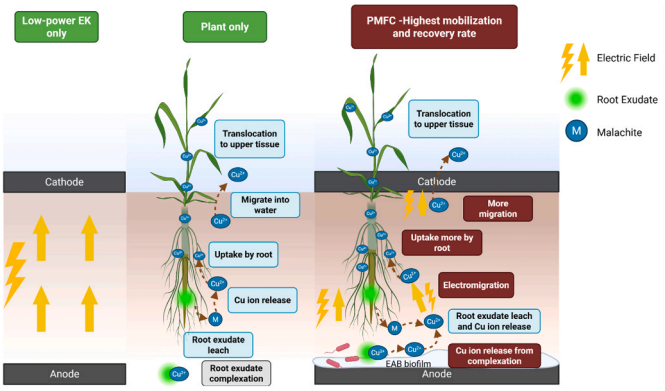

ARTICLE INFO

Keywords:
Plant microbial fuel cells
Recalcitrant copper recovery
Nature-based solution

ABSTRACT

Recovering metals from mineral-bound fractions remains a major challenge because these recalcitrant phases dominate metal-bearing wastes and render much of the metal inaccessible. We employed plant-microbial fuel cells (PMFCs) to mobilise and recover metal from such materials through a combination of mobilisation via root exudate leaching, low-power electrokinetic transport powered by the fuel cell and ultimately plant uptake. Here, we demonstrate that PMFCs can substantially enhance copper mobilisation and recovery from malachite ($Cu_2CO_3(OH)_2$)-spiked soils, as a model of metal-bearing mineral waste, using common reed (*Phragmites australis*). In soil-only systems, copper mobilisation was negligible. Application of low-power electrokinetics alone increased aqueous Cu concentrations only modestly. Plant-only systems enhanced mobilisation via root exudates. By contrast, PMFCs, combining plants with low-power electrokinetics, consistently outperformed both single processes: after two months, copper recovery by the plants reached 6.7 % of the initial load—1.8 times higher than in plant-only systems—with Cu mobilisation levels up to 20-fold greater as indicated by aqueous Cu

* Corresponding authors.
** Corresponding author at: National Key Laboratory of Agricultural Microbiology, Huazhong Agricultural University, Wuhan 430070, PR China.
E-mail addresses: qianh5@cardiff.ac.uk (H. Qian), qyhuang@mail.hzau.edu.cn (Q. Huang), HarbottleM@cardiff.ac.uk (M. Harbottle).

https://doi.org/10.1016/j.jhazmat.2026.141421
Received 18 November 2025; Received in revised form 13 January 2026; Accepted 7 February 2026
Available online 8 February 2026

concentration. These outcomes reveal a clear synergistic effect between root-exudate-driven lixiviation combined with the likely circuit-maintained reducing conditions and field-assisted transport, enabling enhanced recovery of copper from recalcitrant malachite. This study establishes PMFCs as a promising nature-based platform for sustainable remediation and resource recovery from recalcitrant metal-bearing wastes.

1. Introduction

Copper (Cu), aluminium (Al), and zinc (Zn) are critical non-ferrous metals essential for economic and social development [1]. In 2023, global mine production reached about 23 million tonnes of Cu, 69.9 million tonnes of Al, and 11.6 million tonnes of Zn to meet industrial demands [2]. This heavy usage generates greater than 20 billion tonnes of tailings each year, which retain 5–15 % of the various minerals and critical non-ferrous metals that were resident in the parent orebody [3]. Although metal reserves evolve with discoveries and resource-to-reserve reclassification driven by prices and technology [4], average ore grades have declined and environmental burdens have increased. For copper, Delgado [5] estimated that by 2008 ~50 % of known reserves had already been extracted, leaving about 35 years of production at 2008 mining rates [5]. Taken together, large residue streams, declining grades, and higher environmental costs underscore the urgency of sustainable metal recovery from solid wastes.

Conventional metal-recovery routes are effective at industrial scale, routinely processing million-tonnes solid wastes per year [6], but they can be energy- and reagent-intensive and may generate secondary wastes. For example, hydrometallurgical extraction of copper from mining tailings through nitric acid leaching produces highly toxic effluents [7]. Similarly, the Waelz process, a pyrometallurgical technique widely applied to recover Zn and associated metals (Pb and Cu) from metallurgical slags and dusts, operates at temperatures above 1000 °C, resulting in substantial energy consumption and producing secondary solid residues and acidic SO_2 emissions [8]. In contrast, plant-based recovery proceeds much lower throughputs and is positioned as a complementary in situ strategy for low-grade, widely dispersed soils where excavation or harsh reagents are not feasible. For instance, *Pteris vittata* achieved a 26.3 % recovery of arsenic from copper chrome arsenate (CCA) contaminated soils in two years without soil excavation or chemical amendments [9]. *Sedum plumbizincicola* extracted 17 % of the NH_4OAc-extractable Zn from field soils exhibiting a distance-based contamination gradient near a copper smelter over two years, and repeated planting–harvesting enhanced soil microbial functions [10]. These recovery processes involve mechanisms including specific-plant-protein binding, cell-wall adsorption, and movement of metal ions into vacuoles [11]. However, plant uptake typically addresses metals in labile/exchangeable pools rather than mineral-bound fractions. Addressing this gap calls for plant-based approaches that actively enhance mobilisation and directed transport from mineral-bound reservoirs.

Plant microbial fuel cells (PMFCs) combine the potential for phytomobilisation and phytoremediation of metals with the ability to transport ionic species *via* electrokinetic phenomena [12,13]. In PMFCs, plant root exudates provide substrates for electroactive bacteria, which generate electrons during substrate decomposition. These electrons are captured by anodes and transferred to cathodes where electron acceptors (e.g. oxygen) are present, creating a bioelectric circuit powered by redox reactions [14]. Current PMFC research has mainly focused on applying PMFCs for metal ions removal and bioelectricity generation in soils, sediments, sludges, and wastewater [15,16]. PMFCs have achieved removal efficiencies of up to 94 % for Cu (II) in wastewater systems employing algae-supported cathodes [17]. In soil-based applications, a PMFC planted with *Ipomoea aquatica* removed 71.2 % of Cu (II) from paddy soils within 96 days, while systems established with *Pennisetum sinese* accomplished up to 99 % removal of hexavalent chromium from contaminated soils [18]. However, relatively few studies have targeted the mobilisation and recovery of metals from recalcitrant mineral forms, despite the fact that residual or mineral-bound fractions constitute a dominant proportion of the metal in wastes (mining tailing, slags, etc.). For example, in Pb–Zn tailings from the Old Lead Belt, Missouri (USA), most (61–86 %) lead, copper, cadmium and zinc occurs in the residual fraction; and in coal-gasification fine slag from Ningdong, Ningxia (China), most metals are likewise residual-bound (~50–87 %) [8,19].

Theoretically, PMFCs offer two main advantages for this purpose: first, plant root exudates can promote metal leaching through acidification effects caused by dissolved organic acids, and complexation by exuded ligands can promote metal dissolution from solids via ligand-promoted dissolution (LPD) at the mineral–solution interface [20]; second, the self-generated electric field in PMFCs can enhance metal mobility and availability for plant uptake via electromigration. In this study, we applied a PMFC system using common reed (*Phragmites australis*) to recover copper from malachite mineral ($Cu_2CO_3(OH)_2$)-spiked soil as a model mineral waste. Here, "mobilisation" refers to dissolved Cu measured in the overlying water, "uptake" refers to Cu accumulated in plant tissues, and "recovery" refers to plant-based recovery, calculated as total Cu uptake in biomass expressed as a percentage of the initial Cu load. Using matched controls and a full compartment mass balance, this study tests the hypothesis that PMFCs coupling plant processes with the self-generated electric field enhance Cu mobilisation and plant-based recovery from the recalcitrant mineral pool, providing insight into PMFC-enabled, sustainable recovery of recalcitrant mineral-bound metals.

2. Materials and methods

2.1. Soil description

Soil samples were collected from the campus of Huazhong Agricultural University in Wuhan, Hubei Province. After collection, the soil was air-dried and sieved through a 2-mm mesh to remove stones, plant residues, and plastic debris. Soil pH was 6.2 determined in water at a 1:5 (soil: water, w/v) ratio and contained 27.49 g/kg total carbon (TC), 1.98 g/kg total nitrogen (TN), and 0.82 g/kg total phosphorus (TP) [21]. The background Cu concentration was 0.03 mg/g determined by the ICP-OES with mixed acid (2.0 mL HCl, 9.0 mL HNO_3, 3.0 mL HF, and 1.0 mL H_2O_2) digest.

To model a recalcitrant, mineral-bound Cu pool representative of oxidized copper wastes, we spiked soil with malachite ($Cu_2CO_3(OH)_2$; Sangon Biotech, China). Malachite (Cu_2CO_3 $(OH)_2$) is sparingly soluble with log $K_{sp} \approx -33$ at 25 °C [22]. It's also one of the most widely occurring secondary Cu minerals in oxidized zones, making it a realistic proxy for mineral-waste weathering contexts [23].

A preliminary phytotoxicity assay was performed to select a suitable malachite dose for subsequent experiments. Malachite was mixed into dry, sieved soil at 0, 5, 7.5, and 10 mg malachite g^{-1} dry soil (three replicates per treatment). Uniform lateral roots of common reed with comparable initial size (root length/biomass) were transplanted. After 2 weeks, plant responses were assessed by the number of newly formed roots, root lengths, stem lengths, and fresh biomass (Table S1). Based on these indicators, 7.5 mg/g malachite dose was selected resulting in final concentration of 4.44 ± 0.11 mg/g Cu in mixture determined by ICP-OES with mixed acid digest. After dry premixing soil with malachite, deionised water was added to reach a water content of 55 % and the mixture was sealed for 72 h to prevent evaporation and allow porewater diffusion and homogeneous distribution of dissolved constituents (e.g.,

soil electrolytes and dissolved organic carbon); pre-wetting also reduced dust, improved cohesiveness, and facilitated reproducible transfer into experimental tubes.

2.2. Experiment setups and operations

The experimental setup included seven treatments: Cu-PMFC, PMFC, Cu-E, Cu-Plant, Plant, Cu-Soil, and Soil (Fig. 1). The components and objectives of each treatment are summarized in Table 1. Each treatment had six replicates with three destructively sampled after one month (M1) and the remaining sampled after two months (M2). A total of 42 experimental units were assembled in individual acrylic tubes (20 cm in length × 2.2 cm in diameter). Each tube contained 72 g of bulk soil or $Cu_2CO_3(OH)_2$-spiked soil under flooded conditions, with a 15 cm soil column and a 15 mL water layer. The water layer was replenished regularly with DI deionized water; therefore, evaporation did not concentrate Cu and the variations in overlying-water Cu were attributed primarily to mobilisation and diffusion from the sediment. The experiments were conducted in an incubator at a constant temperature of 28°C with a 16/8 h light/dark cycle. Hereafter, treatment groups are referred to as Cu-PMFC, Cu-Plant, Cu-E, Cu-Soil (Cu denotes malachite-spiked systems), PMFC, Plant, and Soil. Sampling timepoints are Month 1 and Month 2 (abbreviated as M1 and M2). Individual experimental replicates are indicated by a trailing index after the timepoint (e.g., Cu-PMFC-M1–1 denotes the Cu-PMFC treatment at Month 1, replicate 1; replicate indices run from 1 to 3).

For the Cu-PMFC, PMFC, and Cu-E treatments, closed electric circuits were established. Graphite plates (0.5 cm height × 2.2 cm diameter) were used as anodes, tightly sealed to rubber bungs with waterproof adhesive to prevent leakage, and then inserted into the tubes. Cathodes consisted of commercial graphite rods (4 cm length × 0.8 cm diameter) connected to the anodes through 1200 Ω resistors with insulated copper wires. In the Cu-E treatment, an external voltage of 100 mV was applied to provide the electric field. Common reeds (*Phragmites australis*) were employed for the Cu-PMFC, PMFC, Cu-Plant, and Plant treatments. Uniform lateral roots (~7 cm in length) with small attached root

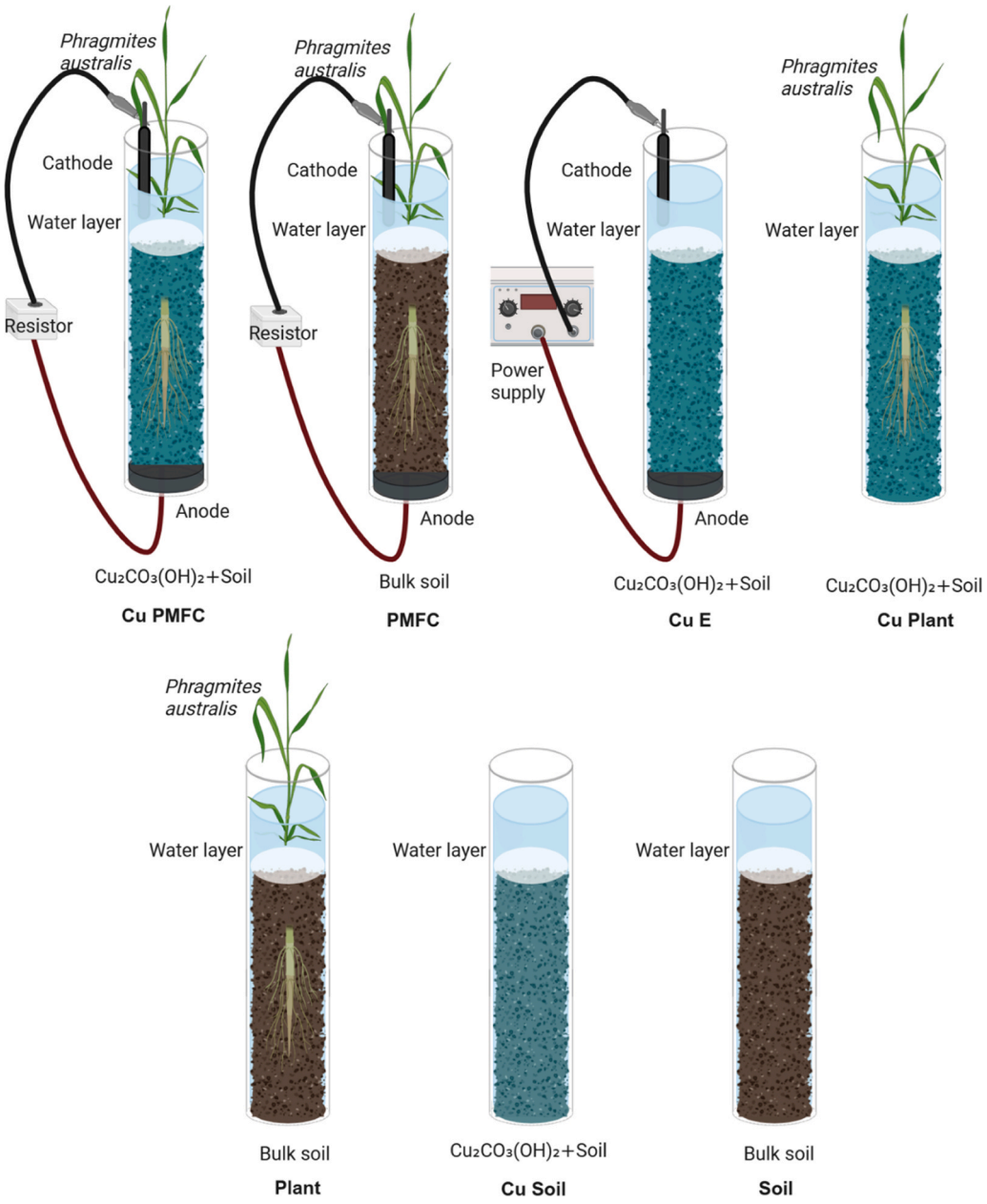

Fig. 1. Experiment setups.

Table 1
Experiment setups description.

Treatment	Conditions				Description
	Plant	PMFC	External field	Malachite	
Cu-PMFC	Y	Y		Y	To explore power generation, plant growth and Cu mobilisation and uptake
PMFC	Y	Y			To explore power generation and plant growth without Cu
Cu-E			Y	Y	To explore effect of low electric field on Cu mobilisation
Cu-Plant	Y			Y	To explore phytoextraction of Cu without other treatment
Plant	Y				Plant growth control
Cu-Soil				Y	To explore leachability of Cu without other treatment
Soil					Negative control

segments from the same or similar parent plants were selected, and each was transplanted 5 cm above the anode. Plant materials were purchased from Tianli Aquatic Plant Cultivation Co., Ltd. (China). For the Cu-PMFC and PMFC treatments, bioelectrical signals were logged continuously using a multichannel data acquisition system (Keysight U2355A) at 10-min intervals. Each experimental unit was assigned two input channels configured for differential measurement; therefore, the recorded voltage represents the potential difference between the cathode and anode ($V = V_{cathode} - V_{anode}$). Current and power under the fixed external load were calculated as $I = V/R$ and $P = V^2/R$ (V in volts). Current density (J) and power density (PD) were obtained by normalising I and P to the geometric anode surface area. The reported current/power density values are derived under the fixed external load (1200 Ω) from the continuous voltage records and are intended for comparative trend analysis between treatments rather than optimisation of maximum power output. No smoothing or filtering was applied to the voltage records; calculations use the recorded values as logged.

When destructively sampling plant-containing replicates (Cu-PMFC, PMFC, Cu-Plant, and Plant), plants were harvested by cutting the aboveground parts, which were stored at 4 °C, while leaving the belowground parts in place. Although roots are also required for subsequent quantitative analysis, their removal at this stage would have caused disturbance within the systems. Therefore, these setups, together with the no-plant controls, were frozen at –20 °C for 24 h to preserve the system integrity in solid form. After complete freezing, the entire samples were carefully pushed out of the acrylic tubes for subsequent separation and analysis.

2.3. Chemical analysis

After intact extrusion from the acrylic tubes, all frozen samples were placed on pre-cooled, clean aluminium foil and sectioned into water layer, topsoil, middle soil, and bottom soil using clean stainless-steel knives. The water layers were rapidly transferred into 50-mL centrifuge tubes, thawed at room temperature, filtered through 0.45-μm membranes, and analysed for Cu concentration using inductively coupled plasma–optical emission spectrometry (ICP-OES; Agilent 5510, Agilent Technologies Inc., USA). The three soil sections of each setup were placed into separate 50 mL centrifuge tubes. For soil samples containing plant tissues, tubes were kept at 4 °C for 30 min to allow partial thawing, after which the tissues were carefully removed with clean tweezers. The separated root tissues were transferred into new centrifuge tubes and cleaned in an ultrasonic bath for 10 min to remove adherent rhizosphere soil. The detached rhizosphere soil was collected and recombined with the corresponding bulk soil samples. All soil samples were subsequently freeze-dried for further analysis.

To determine Cu concentrations in soil samples, microwave-assisted acid digestion was performed prior to ICP-OES analysis. For each sample, 0.25 g of finely ground soil (<0.149 mm) was digested with a mixed-acid solution consisting of 2.0 mL HCl, 9.0 mL HNO_3, 3.0 mL HF, and 1.0 mL H_2O_2 using a MARS microwave digestion system [24]. The digestion program was as follows: the temperature was increased to 180 °C within 15 min, maintained for 30 min, and then allowed to cool to room temperature over 30 min. The digests were diluted to a final volume of 25 mL with deionized water and analysed for Cu concentration by ICP-OES.

Because malachite was dispersed within a heterogeneous soil matrix after the experiment, we quantified Cu using compartment mass balance and total digestion–ICP-OES rather than attempting bulk mineralogical/valence-state characterisation of solid Cu phases.

2.4. Plant analysis

Plant samples were separated into roots, stems, and leaves. The samples were then oven-dried at 75 °C to constant weight, and dry biomass was measured. Dried tissues were finely ground into powder using a high-throughput tissue grinder for subsequent analysis. Plant powders (0.25 g) were digested with mixed acids (9 mL HNO_3 and 3 mL H_2O_2) in a MARS microwave digestion system [25]. The digestion program was the same above. The digests were diluted to a final volume of 25 mL with deionized water and analysed for Cu concentration by ICP-OES.

2.5. Analytic methods

Principal component analysis (PCA) was performed in R (version 2022.07.2) using stats package, and the results were visualized with the factoextra package [26] to identify major variance patterns among treatments and replicates.

To assess the internal redistribution of metals within plants, the translocation factor (TF) was calculated as (2):

$$TF = C_{shoot}/C_{root} \quad (2)$$

Where C_{shoot} and C_{root} represent the metal concentrations in the aboveground tissues and roots, respectively. TF-Stem and TF-Leaf refer to C_{stem}/C_{root} and C_{leaf}/C_{root}. A $TF > 1$ indicates effective translocation of metals from roots to shoots, while $TF < 1$ reflects preferential retention in roots [27,28].

Statistical analysis was performed using one-way ANOVA with Tukey's Honestly Significant Difference (HSD) test at a significance level of $p < 0.05$. Correlation analysis was performed using Spearman analysis at a significance level of $p < 0.05$. Because organ biomasses were highly collinear (Spearman $r \approx 0.99$, $p < 0.0001$), and mechanistically, Cu uptake occurs at the root–soil interface, the linear fittings between root biomass and Cu uptake by roots, stems, and leaves in Cu-PMFC and Cu-Plant treatments were analysed to explore the potential role of plant growth in driving Cu accumulation.

3. Results

3.1. PMFC voltage generation

Voltage generation was highly variable both over time and among replicates. To transparently show this variability, voltage time series from individual experimental units are presented in Fig. 2a and b, and the corresponding mean ± SD (n = 3) trends are summarised in Fig. 2c and d. Derived current density and power density calculated from the voltage records are provided in the Supporting Information (Table S2;

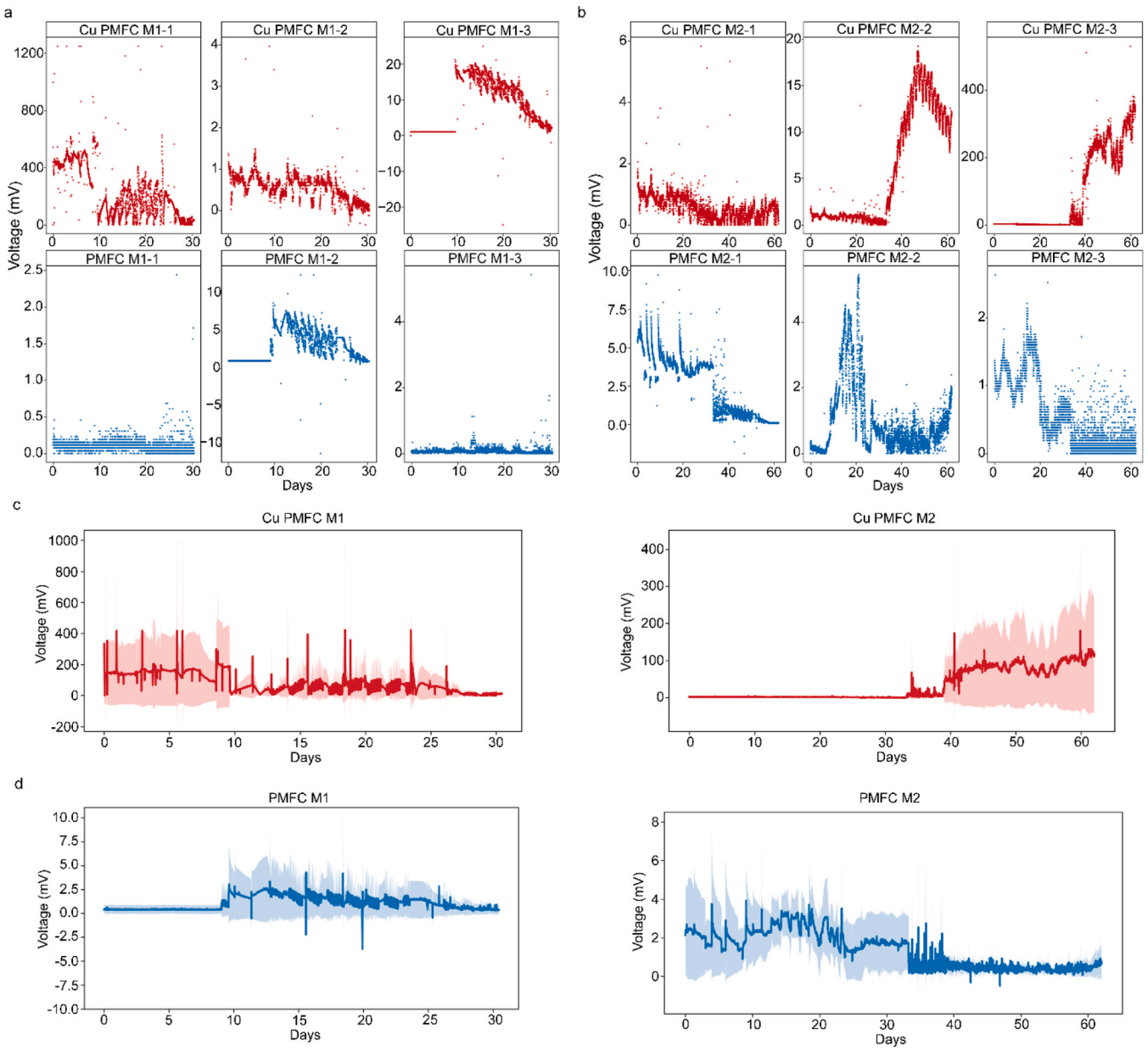

Fig. 2. Voltage generation of Cu PMFC and PMFC setups. (a) Voltage time series of individual replicates (n = 3) in M1; each subplot represents one device. (b) Voltage time series of individual replicates (n = 3) in M2. (c) Mean voltage ± SD (n = 3) for Cu PMFC in M1 (left) and M2 (right). (d) Mean voltage ± SD (n = 3) for PMFC in M1 (left) and M2 (right). Voltages were recorded across a 1200 Ω external resistor under closed-circuit conditions.

Figs. S1–S2). In certain replicates (e.g., PMFC-M1–1), voltage outputs were close to zero with only small-amplitude fluctuations. Cu-PMFC replicates generally produced higher voltages, with four of the six units exhibiting sustained outputs > 10 mV and two exceeding 100 mV, whereas none of the PMFC units exceeded 10 mV. This variability may in part reflect differences in colonization and development of electroactive microbial communities at the bioanode. Even among individuals of the same plant species, natural variation in root exudate composition under the identical surrounding has been reported [29]. This potential differences in exudate profile might directly alter substrate availability, influence the establishment and activity of electroactive bacteria, and ultimately contribute to the divergent voltage outputs observed among replicates.

In most replicates, small cyclic fluctuations were observed, likely corresponding to diurnal cycles, as the average interval between voltage peaks was approximately 24 h (Fig. 2a and b). In some replicates (e.g., Cu-PMFC-M1–3 and Cu-PMFC-M2–2), voltage output declined in the later stages, which may indicate depletion of available carbon sources in the growth medium.

3.2. Plant biomass and uptake of copper

Plant dry biomass varied over time, with considerable replicate-to-replicate differences in M1 (Fig. 3a). After M2, PMFC replicates without Cu remained highly inconsistent, with one replicate (M2–1) exhibiting the lowest total dry biomass (1.84 g) and showing blackened, decayed roots that coincided with a marked voltage decline and eventual cessation (Figs. 2b and 3b). By contrast, there was generally more agreement among replicates in other treatments (Fig. 3b). Overall, greater biomass was observed in Cu-PMFC and particularly in Cu-Plant treatments compared with the plant-only controls.

Biomass Cu concentrations (Table S3) were relatively consistent across replicates despite the variability in biomass noted earlier. Overall, Cu was retained primarily in roots, followed by stems with only minimal

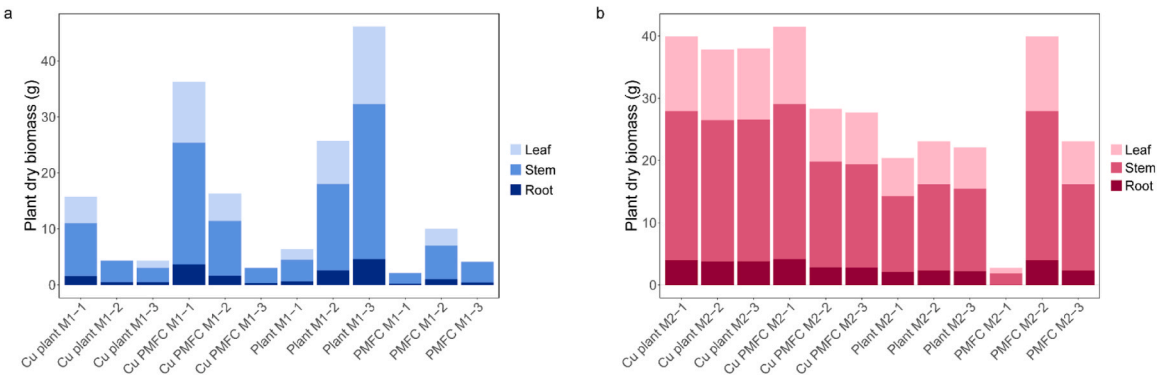

Fig. 3. Plant dry biomass of each Cu Plant, Cu PMFC, Plant, and PMFC setup in M1 (a) and M2 (b).

concentrations in leaves, with all TF values remaining below 1. According to ANOVA with HSD tests, significant differences were only detected between replicates in roots and stems (Fig. 4a, b). Root Cu concentration was broadly similar in Cu-Plant and Cu-PMFC after M1 (Fig. 4a). In M2, however, a clear divergence emerged: root Cu concentrations in Cu-Plant declined significantly, while those in Cu-PMFC significantly increased approximately threefold, (Table S3, Fig. 4a). Stem Cu concentrations showed no treatment differences, but both treatments exhibited significant decreases in M2 (Fig. 4b), consistent with reduced translocation from roots to stems (Fig. 4c). The significantly decreased translocation of Cu from roots to stems in Cu-Plant and Cu-PMFC after M2 implied the Cu exposure-induced stress response (Fig. 4c). The low Cu concentrations observed in tissues from treatments without copper addition confirmed the naturally low background levels of Cu in common reeds (Table S3, Fig. 4a, b).

When biomass was taken into account to calculate the total Cu mass in each compartment (Fig. 5a, b), these trends persisted. After M2, Cu mass was significantly higher in Cu-PMFC treatments compared to Cu-Plant treatments, with PCA of M2 revealing a clearer separation between Cu-PMFC and Cu-Plant than in M1 (Fig. 5c, d). It is also notable that there was a greater proportion of the Cu mass in the stems after M1, and a greater proportion in the roots after M2. ANOVA with HSD test further revealed that Cu mass uptake by roots in the Cu-PMFC-M2 was significantly greater than other treatments ($p = 0.01$; Fig. 5e), whereas no significant differences in Cu mass uptake by leaves or stems were observed across the setups (Fig. 5f, g).

3.3. Copper in soil and water

Fig. 6 showed the copper concentrations in both soil and overlying water layers for all malachite-containing setups in M1 and M2. The initial Cu concentration in the malachite-spiked soil was 4.44 mg/g. In M1, the Cu-Soil and Cu-E systems maintained relatively consistent soil Cu levels (Fig. 6a), whereas both Cu-Plant and Cu-PMFC systems showed significantly reduced concentrations. Notably, Cu in Cu-PMFC topsoil decreased by 7–11 % relative to the initial spike, while the other systems fluctuated within ±4.5 %, with Cu-PMFC topsoil recording the lowest values (3.95–4.13 mg/g). By M2, more pronounced variations emerged across all systems. In Cu-Soil, Cu was significantly enriched in the bottom layer (4.52–4.58 mg/g), whereas in Cu-E and Cu-Plant, the highest values were detected in the middle layer (4.53–4.78 mg/g and 3.95–4.60 mg/g, respectively). In contrast, Cu-PMFC exhibited a clear vertical gradient, with concentrations decreasing from top to bottom by ~16 %.

Water-layer Cu concentrations were generally low across all systems, yet provided evidence of Cu migration (Fig. 6c, d). In Cu-Soil, water concentrations were minimal (0.013–0.015 mg/L in M1; 0.011–0.040 mg/L in M2), consistent with the low solubility of malachite. Cu-E showed slightly higher levels (0.021–0.078 mg/L in M1; 0.040–0.080 mg/L in M2), which may reflect mobilisation of a small proportion of labile Cu fraction by low voltages. In Cu-Plant, concentrations were further elevated (0.124–0.198 mg/L in M1; 0.070–0.592 mg/L in M2), likely reflecting the leaching effect of root exudates. Cu-PMFC consistently had the highest water-layer Cu concentrations: 0.264–0.965 mg/L in M1 (2.1–4.9 times higher than Cu-Plant, 12–13 times than Cu-E, and 20–64 times than Cu-Soil) and 1.420–2.893 mg/L in M2 (4.9–20.3times higher than Cu-Plant, 36 times than Cu-E, and 72–129 times than Cu-Soil). These data indicated that Cu mobilisation in Cu-PMFC was potentially driven by the synergistic effects of root exudate leaching and electromigration of Cu ions from

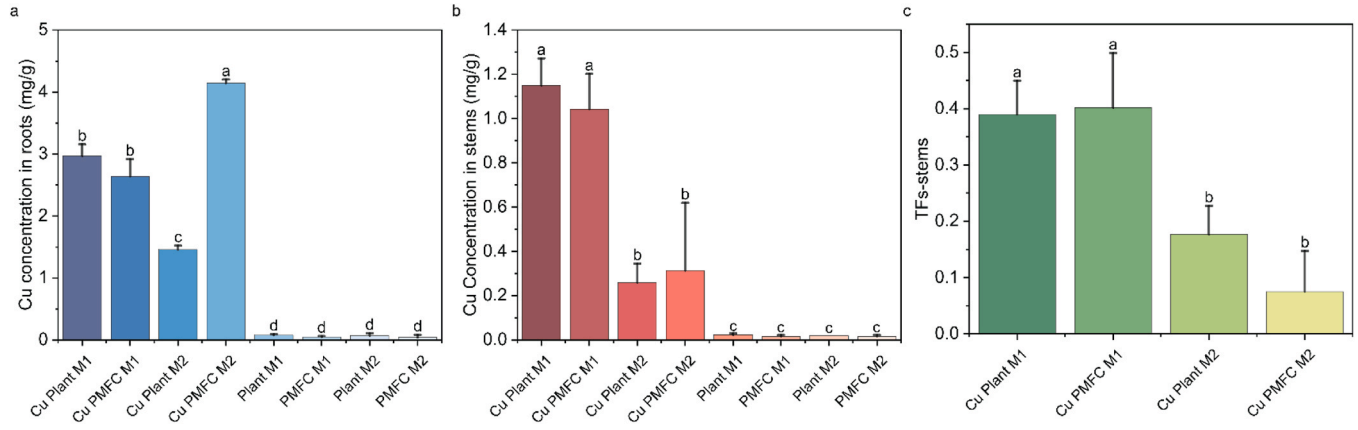

Fig. 4. Significant differences of Cu concentrations in roots (a) and stems (b) among Cu Plant, Cu PMFC, Plant, and PMFC setups in M1 and M2. Significant differences of translocation factor of Cu from roots to stems (TF-stems) among above setups was shown in c. Comparisons were based on ANOVA with HSD tests.

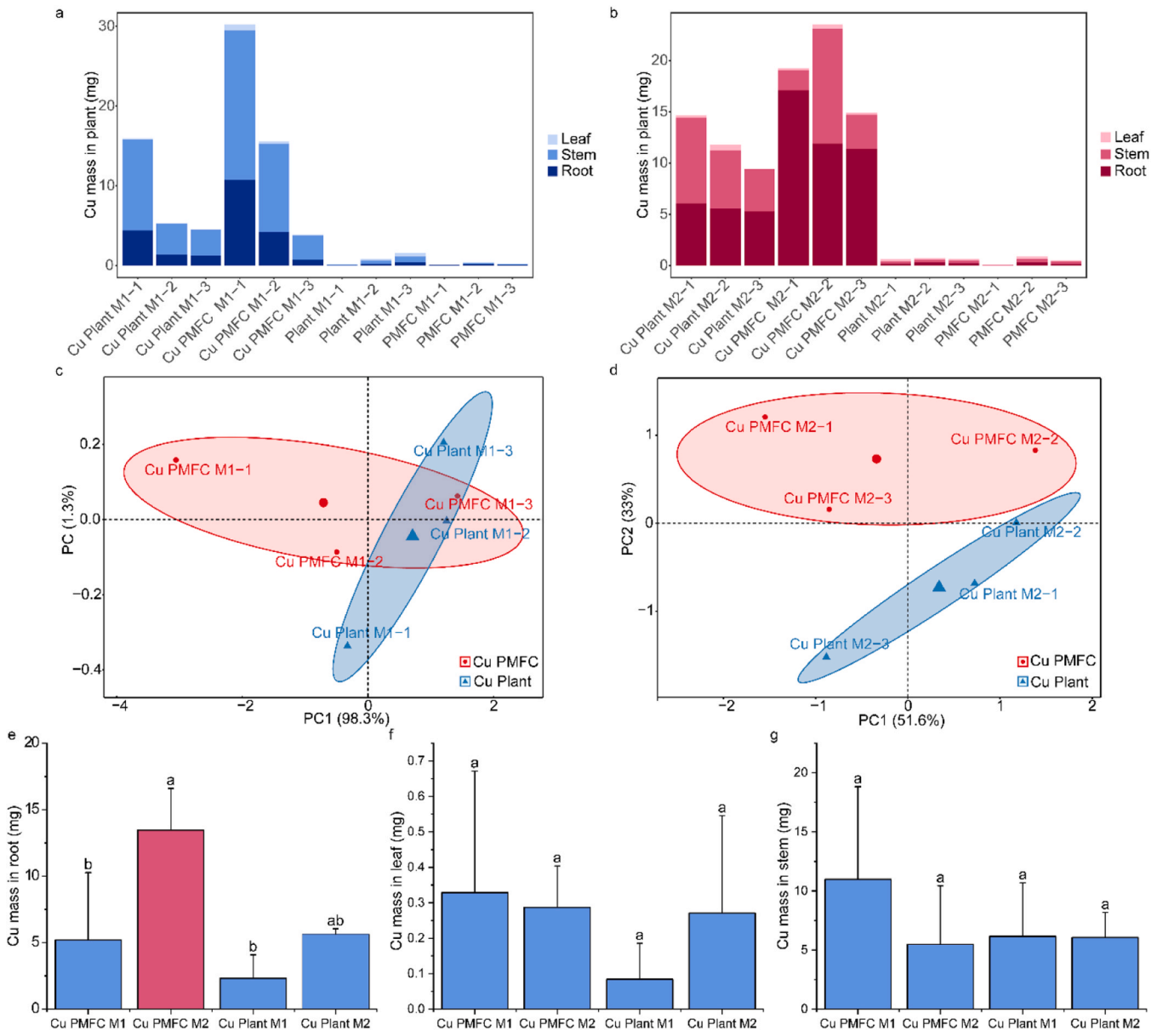

Fig. 5. Copper mass in leaf, stem, and root of Cu Plant, Cu PMFC, Plant, and PMFC treatments in M1 (a) and M2 (b). PCA analysis between Cu Plant and Cu PMFC of M1 (c) and M2 (d) was based on the copper mass. ANOVA with HSD tests were performed in Cu mass of plant root (e), leaf (f), and stem (g) among Cu PMFC M1, M2, and Cu Plant M1, M2. Different letters represented significant difference, and the same letters represented insignificant differences among groups.

anode to cathode.

PCA provided an integrated view of these patterns, showing Cu-PMFC as a distinct cluster relative to other systems, consistent with greater Cu disturbance in soils and enhanced migration into water (Fig. 6e, f). Cu-Plant also formed a separate cluster in M1, though this distinction was not evident in M2, while Cu-E and Cu-Soil largely overlapped.

3.4. Copper recovery rate

The initial Cu mass in $Cu_2CO_3(OH)_2$-spiked soil was 320 ± 8 mg, and the Cu mass in soil, water, and biomass compartments was expressed as a percentage of this value to establish the mass balance (Table 2). Mass balance closure was satisfactory, ranging from 96.7 % to 101.2 % of the initial input. The results confirmed the low proportion of Cu in the water layer and were consistent with the trends described above. After two months, Cu-PMFC achieved the highest Cu uptake, with 4.53 % in roots, 2.05 % in stems, and 0.10 % in leaves, corresponding to a total of 6.68 % recovery—1.79 times that of the Cu-Plant system.

4. Discussion

Malachite ($Cu_2CO_3(OH)_2$) is one of the major secondary copper minerals that can be leached by both inorganic and organic lixiviants—such as sulfuric, nitric and hydrochloric acids, as well as citric and malic acids—to release Cu^{2+} [30–32]. In this study, Cu mobilisation in saturated soil only (Cu-Soil specimens) was minimal (Fig. 6c, d). Applying low-power electrokinetics (Cu-E) modestly enhanced mobilisation, with Cu concentrations in water layer up to ~7-fold higher than in the Cu-Soil control in both M1 and M2. However, this effect was still limited relative to the treatments containing plants, where root exudates appear to be a key driver of copper dissolution and availability.

Root exudates mainly comprise sugars, amino acids and carboxylic acids [33]. Among these, low-molecular-weight carboxylates such as malic and citric acids act as natural lixiviants capable of leaching malachite [31,32]. In the Cu-Plant specimens, mobilisation of Cu is expected

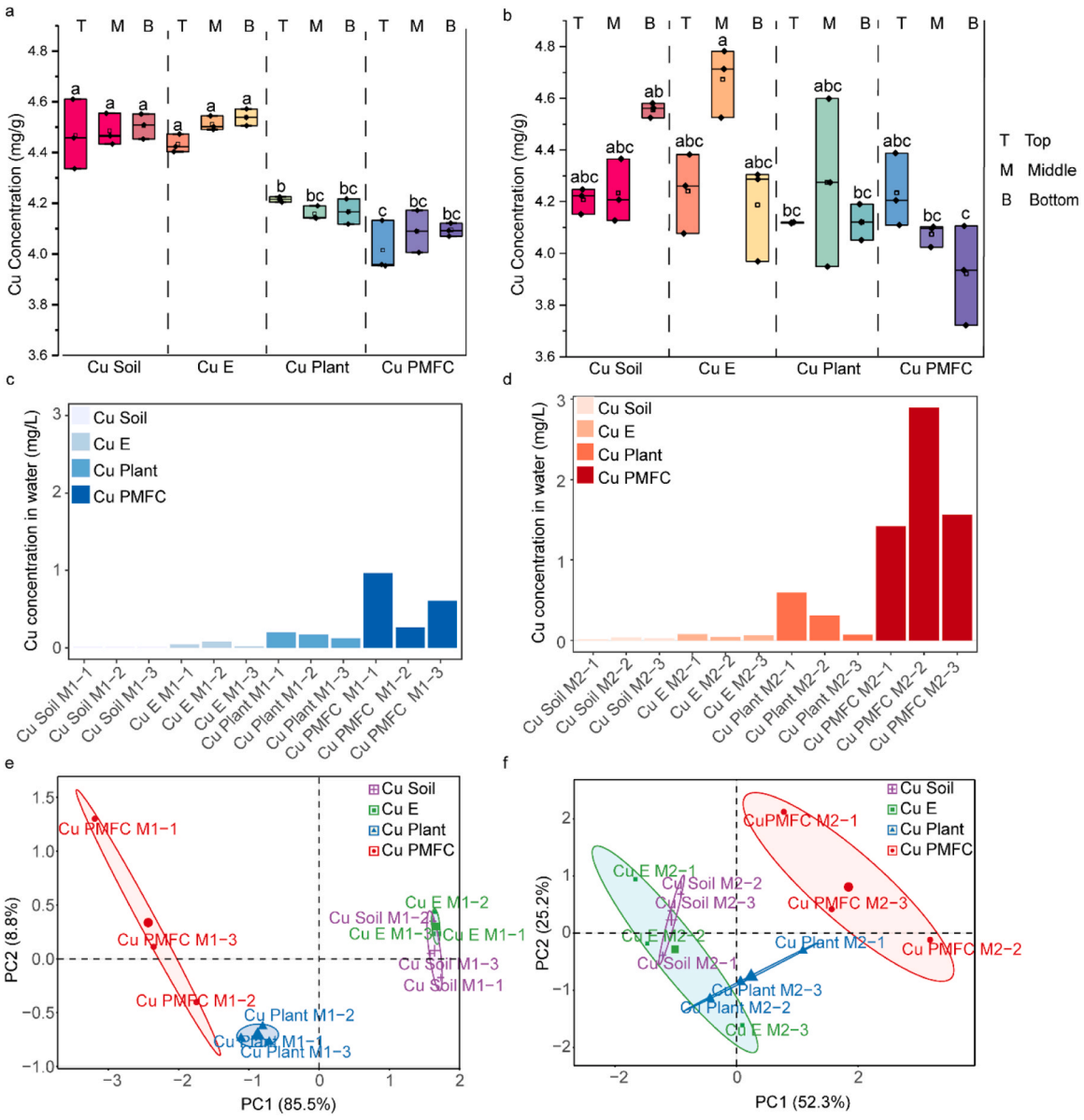

Fig. 6. Copper concentration in soil layers in M1 (a) and M2 (b); copper concentration in water layer in M1 (c) and M2 (d); PCA analysis among Cu soil, Cu E, Cu Plant, and Cu PMFC in M1 (e) and M2 (f) was based on the copper concentration in water layer and soil layers.

Table 2
The mass balance of each system with malachite-spiked soil.

Treatment	Water layer (%)	Upper soil (%)	Middle soil (%)	Bottom soil (%)	Root uptake (%)	Stem uptake (%)	Leaf uptake (%)	Total uptake (%)	Mass balance (%)
Month 1									
Cu-PMFC	0.003	30.12	30.68	30.72	1.63	3.43	0.15	5.21	96.73
Cu-Plant	0.0008	31.63	31.20	31.27	0.73	1.93	0.03	2.69	96.79
Cu-E	0.0002	33.26	33.85	34.05	/	/	/	/	101.17
Cu-Soil	0.00007	33.52	33.65	33.80	/	/	/	/	100.97
Month 2									
Cu-PMFC	0.01	31.88	30.46	29.37	4.53	2.05	0.10	6.68	98.40
Cu-Plant	0.0015	30.90	32.07	30.92	1.76	1.90	0.08	3.74	97.64
Cu-E	0.0002	31.82	35.06	31.41	/	/	/	/	98.30
Cu-Soil	0.0001	31.56	31.76	34.18	/	/	/	/	97.51

to have been enhanced by this root-exudate–driven dissolution, helping to explain the increased Cu available in overlying water after M1 when compared to no-plant specimens. However, the rate of uptake decreased with time, where the concentration of Cu in biomass had decreased after M2 (Table S3, Fig. 4a, b). Statistically, root mass was significantly and negatively linearly correlated with Cu concentrations in roots and stems (R^2 = 0.9740; 0.8724) (Fig. 7d, f). Turning from dissolution to uptake, root acquisition depends on membrane-proximal speciation with free

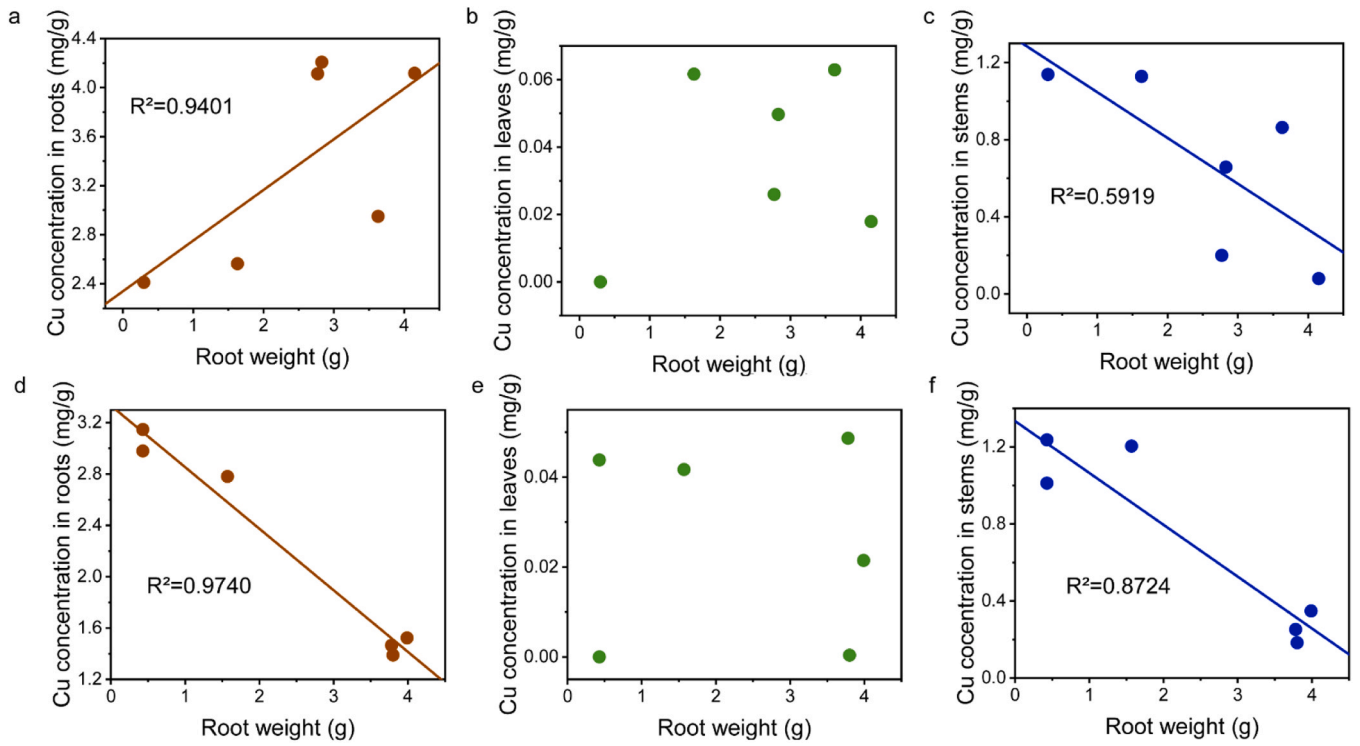

Fig. 7. Linear fitting and no direct correlation between root dry biomass and copper concentrations in roots (a), leaves (b), and stems (c) in Cu PMFC systems. Linear fitting and no direct correlation between root dry biomass and roots (d), leaves (e), and stems (f) in Cu Plant systems.

Cu^{2+} and enzymatic reduction of Cu(II) to Cu(I) for COPT/Ctr import [34]. The significantly reduced root-to-stem translocation of Cu in both Cu-Plant and Cu-PMFC after M2 is consistent with Cu-induced stress responses that retain Cu in roots via cell-wall binding and vacuolar sequestration and restrict xylem loading (Table S3, Fig. 4c) [35]. Under Cu exposure, increased exudation (citrate, succinate, etc.) promotes mineral dissolution but complexes with Cu that reduce free Cu^{2+} and constrain uptake [36–38]. Additionally, the rate of Cu solubilisation may change over time - root age is known to affect exudation [39,40] and as the rhizosphere developed the relative mass of young root material to older material may have decreased, hence changing the exudation pattern. The rate of biomass growth may also change, and increased biomass growth versus decreased Cu uptake would cause a dilution effect. Consistent with Fig. 3, PMFC operation was associated with higher plant dry biomass relative to the plant-only system. The higher plant dry biomass observed under PMFC operation (Fig. 3) can be interpreted in the context of prior PMFC studies linking plant morphological development to PMFC performance. A larger root system and greater shoot biomass generally increase the supply of rhizodeposits, which can potentially promote electroactive biofilm establishment and enhance electricity generation [41]. In particular, Rusyn et al. [42] reported that PMFCs based on *Carex hirta*—the plant with the largest accumulated dry leaf/stem and root mass among the tested species—delivered the highest power output, and they concluded that root-system type and the extent of above-ground photosynthetic surface are useful prognostic factors for PMFC efficiency. The underlying biomass–rhizodeposition–electrogenesis linkage provides a mechanistic framework to interpret plant growth trend: greater biomass under PMFC operation is consistent with stronger rhizosphere activity and could help sustain the bioanode community that underpins the circuit-driven component of Cu mobilisation/recovery [42].

After ~35–40 days under the PMFC circuit, current increased markedly in Cu-PMFC-M2–2 and Cu-PMFC-M2–3 (Fig. S1; Fig. 2b), consistent with the establishment of electroactive microbial activity at the anode, as commonly observed in soil- and plant-based MFCs [41,43,44]. To contextualise the electrokinetic driving potential generated in our PMFCs, we derived current density and power density from the recorded voltages under a fixed external load (R = 1200 Ω; Table S2; Figs. S1–S2). Electricity generation was highly heterogeneous: in Cu-PMFC, J_mean and PD_mean ranged from 0.64 to 269 mA/m^2 and 4.65×10^{-4}–102 mW/m^2 at Month 1, and 0.66–104 mA/m^2 and 5.39×10^{-4}–25.4 mW/m^2 at Month 2, with occasional transient V_max excursions in Cu-PMFC-M1–1 and Cu-PMFC-M2–3 (Table S2). These excursions were short-lived, typically spanning one (occasionally two) logging intervals, and did not correspond to sustained shifts in the underlying time-series trends. A recent compact “biobattery” PMFC designed for power delivery (shortened interelectrode distance of 1 cm and stacked modules) reported maxima of 407 mA/m^2 and 188.33 mW/m^2 [45]. Such higher outputs are achieved by reducing electrode spacing, increasing effective cathode area, and stacking modules. Direct comparison should be treated cautiously because geometry, loading and normalisation conventions (plant growth area vs anode area here) differ across studies. Nevertheless, the sustained non-zero electricity generation in our systems suggests an electrically mediated, low-intensity ion-transport component that may complement root-exudate-driven dissolution and could plausibly contribute to the enhanced Cu mobilisation/recovery observed relative to the controls.

In addition to enhanced dissolution, redox processes could also influence Cu speciation at/near the rhizoplane, such that a fraction of Cu (II) may be transiently reduced to Cu(I) through electron transfer associated with microbial metabolism of exudates and/or root-surface cupric reductases [34]. However, Cu valence/speciation was not directly measured in this study; therefore, any proposed Cu redox/speciation shift remains mechanistically plausible but speculative. Although radial oxygen loss (ROL) creates micro-oxic niches around roots [46], the bulk flooded matrix remains reducing because O_2 diffusion in water is orders of magnitude slower than in air and microbial respiration rapidly exhausts dissolved O_2 [47]. Relative to plant-only systems, the circuit and cathode of PMFCs continuously drain electrons from the anode biofilm, maintaining a low anode potential [48]. This, in turn, likely sustained a

reducing microenvironment in the bioanode/rhizosphere. Biodegradation of root exudates at the bioanode may further liberate Cu from organic complexes and increase its bioavailable fraction, which may explain the moderate rises in aqueous Cu observed even in low-current replicates such as Cu-PMFC-M2–1 (Figs. 2b, 6d).

After 2 months, biomass Cu concentrations were substantially higher in Cu-PMFC than in Cu-Plant across all specimens (Table S3; Figs. 4a, 5b), indicating that circuit activity facilitated its assimilation into plant. Correspondingly, in PMFCs root mass was positively correlated with root Cu ($R^2 = 0.9401$) and negatively correlated with stem Cu ($R^2 = 0.5919$), with no detectable relationship in leaves (Fig. 7a–c). This correlation pattern — together with the markedly elevated root Cu in Cu-PMFC-M2 (Fig. 4a) — implied electromigration sustaining Cu availability at the root–soil interface, thereby strengthening root accumulation although shootward transfer remained constrained. Notably, the PMFC-induced increase in Cu assimilation did not scale with current output: within Cu-PMFC-M2 replicates, root and stem concentrations remained broadly similar regardless of current magnitude (Table S3, Figs. 2b, 4a, b). This finding is consistent with earlier reports that electricity output in PMFCs does not solely dictate metal uptake efficiency at the tissue level [49]. Instead, once additional Cu is mobilised by the circuit, its assimilation into biomass is governed by plant physiological processes. These include membrane transport mediated by specific Cu transporters and metal-uptake/chaperone networks, as well as internal sequestration and compartmentation via phytochelatin production and vacuolar storage, which together determine tissue retention [50,51].

The PMFC treatment (Cu-PMFC) outperformed both phytoremediation alone (Cu-Plant) and low-power electrokinetics alone (Cu-E) in terms of copper mobilisation and plant-based recovery. After two months, Cu-PMFC achieved 6.68 % recovery compared with 3.74 % in Cu-Plant (Table 2). With Cu mobilisation (measured as Cu concentration in overlying water layer), it is possible to demonstrate a clear synergistic effect of the PMFC treatment beyond the combined effect of the plant and electric field. To quantify this for mobilisation, we estimated the expected combined concentration, C_{add}, by adding the effect of the plant only to that of the electric field only and the baseline soil concentration, giving:

$$C_{\mathrm{add}} = (C_{\mathrm{Cu-Plant}} - C_{\mathrm{Cu-Soil}}) + (C_{\mathrm{Cu-E}} - C_{\mathrm{Cu-Soil}}) + C_{\mathrm{Cu-Soil}}$$

At Month 2, C_{add} was 0.07–0.66 mg/L, whereas Cu-PMFC water-layer Cu was 1.42–2.89 mg/L, demonstrating a strongly synergistic enhancement beyond the summed individual contributions. These findings provide a proof-of-concept in malachite-spiked soils, and further validation on well-characterised recalcitrant metal-bearing wastes (e.g., tailings and slags) is required to assess field applicability.

Looking ahead, translating the synergy observed in malachite-spiked soil to real tailings/slags will hinge on several practical constraints. In many tailings/slags, Cu is dominated by mineral-bound phases, and may reside largely in primary sulfides (e.g., chalcopyrite) that are widely regarded as recalcitrant to leaching [52,53]; in such cases, the dissolution step could be even more limiting than in the malachite proxy used here. Against this backdrop, three additional constraints become critical: (i) long-term plant viability—in non-benign wastes, nutrient limitation, metal toxicity and poor structure may suppress root activity and rhizodeposition, intermittently starving the bioanode and weakening the electrical driving force, finally reducing the stability of mobilisation and recovery over months; (ii) matrix heterogeneity—variability in mineralogy and permeability can create strongly driven zones alongside weakly driven zones, increasing scatter between replicates and limiting whole-matrix recovery; and (iii) waste chemistry—dissolved solids and co-existing ions can shift Cu partitioning towards less bioavailable forms *via* complexation, re-adsorption, secondary precipitation and lower effective Cu activity due to increased ionic competition, while also increasing ionic stress that constrain long-term plant performance. At larger scales, these limitations are likely to be amplified by longer transport distances and more pronounced spatial variability. These constraints define the key next step: to establish the operating envelope of PMFC-assisted mobilisation and recovery in well-characterised tailings/slags by tracking long-term plant condition, verifying dissolution-limited behaviour for recalcitrant pools, and assessing spatial robustness across realistic heterogeneous matrices.

5. Conclusion

This study provides new evidence that PMFCs can promote copper mobilisation and recovery from recalcitrant malachite-spiked soils. After two months, Cu recovery in PMFC specimens reached 6.68 % of the initial load, nearly twice that of Cu-Plant (plant-only control in malachite-spiked soil; no circuit) (3.74 %), with aqueous Cu concentrations 4.9–20 times higher than in Cu-Plant and ~36 times higher than in Cu-E (low-power electrokinetic control in malachite-spiked soil; circuit applied but no plants) treatments. These outcomes reflect a synergy between root-exudate-driven dissolution and circuit-induced ion transport, with the circuit likely maintaining a reducing microenvironment and elevated Cu availability at the root–soil interface; potential Cu redox/speciation shifts are plausible but were not directly resolved here. Although current magnitude might not directly dictate uptake efficiency, the presence of the circuit was essential in maintaining elevated Cu availability. Together, these findings demonstrated that PMFCs can overcome limitations of conventional phytoremediation and electrokinetics, offering a sustainable route for recovering metals from otherwise inaccessible mineral-bound fractions in soils and tailings.

Environmental implication

Recovering recalcitrant heavy metal in waste typically requires harsh chemicals/high energy input. This study shows PMFCs can synergistically mobilise and recover Cu from recalcitrant malachite by coupling root-exudate lixiviation with circuit-induced ion transport. After two months, PMFCs achieved 6.68 % recovery—1.80 times higher than that of plant-only systems. Crucially, the driving electricity is generated in situ from rhizodeposits via microbial metabolism, so external energy demand is minimal and operation can be potentially near energy-neutral. Coupling root-exudate–driven solubilisation with circuit-induced ion transport overcame limitations of phytoremediation/electrokinetics used alone. Together, PMFCs offer a promising, nature-based route for valorising recalcitrant metal-bearing wastes.

CRediT authorship contribution statement

Wenli Chen: Writing – review & editing. **Devin Sapsford:** Writing – review & editing, Methodology, Conceptualization. **Michael Harbottle:** Writing – review & editing, Supervision, Conceptualization. **Qiaoyun Huang:** Writing – review & editing, Resources, Conceptualization. **Zhenghui Gao:** Writing – review & editing. **Hang Qian:** Writing – review & editing, Writing – original draft, Methodology, Investigation, Formal analysis, Conceptualization.

Declaration of Generative AI and AI-assisted technologies in the writing process

During the preparation of this work the authors used Chatgpt in order to polish language. After using this tool, the authors reviewed and edited the content as needed and take full responsibility for the content of the published article.

Declaration of Competing Interest

No conflict. The authors declare that they have no known competing financial interests or personal relationships that could have appeared to influence the work reported in this paper.

Acknowledgement

We gratefully acknowledge financial support from the China Scholarship Council (CSC) for Hang Qian (CSC No. 202106760089). We sincerely acknowledge for the help of Dr. Yu Cao and Dr. Tao Chen from Wuhan Botanic Garden (Chinese Academy of Sciences) and Hainan University for advice and support in carrying out the experiments.

Appendix A. Supporting information

Supplementary data associated with this article can be found in the online version at doi:10.1016/j.jhazmat.2026.141421.

Data availability

Data will be made available on request.

References

[1] Cusano, G., Rodrigo Gonzalo, M., Farrell, F., Remus, R., Roudier, S., Delgado Sancho, L., 2017. Best Available Techniques (BAT) Reference Document for the Non-Ferrous Metals Industries. Industrial Emissions Directive 2010/75/EU (Integrated Pollution Prevention and Control). Joint Research Centre.
[2] Idoine, N., Raycraft, E., Hobbs, S., Everett, P., Evans, E., Mills, A., et al., 2025. World Miner Prod 2019–2023.
[3] Abbadi, A., Mucsi, G., 2024. A review on complex utilization of mine tailings: recovery of rare earth elements and residue valorization. J Environ Chem Eng 12, 113118.
[4] Ash, S., 2019. Mineral commodity summaries 2019. US Geological Survey Reston, VA.
[5] Delgado, A.V., 2014. Mineral resource depletion assessment. Eco-efficient Construction and Building Materials. Elsevier, pp. 13–37.
[6] Antuñano, N., Cambra, J.F., Arias, P.L., 2019. Hydrometallurgical processes for Waelz oxide valorisation – An overview. Process Saf Environ Prot 129, 308–320.
[7] Peelman, S., Sun, Z.H., Sietsma, J., Yang, Y., 2016. Leaching of rare earth elements: review of past and present technologies. Rare earths Ind 319–334.
[8] Guo, Y., Zhang, Y., Zhao, X., Xu, J., Qiu, G., Jia, W., et al., 2022. Multifaceted evaluation of distribution, occurrence, and leaching features of typical heavy metals in different-sized coal gasification fine slag from Ningdong region, China: a case study. Sci Total Environ 831, 154726.
[9] Kertulis-Tartar, G., Ma, L., Tu, C., Chirenje, T., 2006. Phytoremediation of an arsenic-contaminated site using Pteris vittata L.: a two-year study. Int J Phytoremediat 8, 311–322.
[10] Jiang, J., Wu, L., Li, N., Luo, Y., Liu, L., Zhao, Q., et al., 2010. Effects of multiple heavy metal contamination and repeated phytoextraction by Sedum plumbizincicola on soil microbial properties. Eur J Soil Biol 46, 18–26.
[11] Hussain, I., Afzal, S., Ashraf, M.A., Rasheed, R., Saleem, M.H., Alatawi, A., et al., 2023. Effect of metals or trace elements on wheat growth and its remediation in contaminated soil. J Plant Growth Regul 42, 2258–2282.
[12] Habibul, N., Hu, Y., Sheng, G.-P., 2016. Microbial fuel cell driving electrokinetic remediation of toxic metal contaminated soils. J Hazard Mater 318, 9–14.
[13] Sun, Y., Wang, H., Long, X., Xi, H., Biao, P., Yang, W., 2022. Advance in remediated of heavy metals by soil microbial fuel cells: mechanism and application. Front Microbiol 13, 997732.
[14] Yan, X., Lee, H.-S., Li, N., Wang, X., 2020. The micro-niche of exoelectrogens influences bioelectricity generation in bioelectrochemical systems. Renew Sustain Energy Rev 134, 110184.
[15] Oon, Y.-L., Ong, S.-A., Ho, L.-N., Wong, Y.-S., Oon, Y.-S., Lehl, H.K., et al., 2015. Hybrid system up-flow constructed wetland integrated with microbial fuel cell for simultaneous wastewater treatment and electricity generation. Bioresour Technol 186, 270–275.
[16] Wang, X.T., Cui, X.Q., Fang, C., Yu, F., Zhi, J.A., Masek, O., et al., 2022. Agent-assisted electrokinetic treatment of sewage sludge: heavy metal removal effectiveness and nutrient content characteristics. Water Res 224, 11.
[17] Das, S., Kumar, S., Mehta, A.K., Ghangrekar, M.M., 2024. Heavy metals removal by algae and usage of activated metal-enriched biomass as cathode catalyst for improving performance of photosynthetic microbial fuel cell. Bioresour Technol 406, 131038.
[18] Guan, C.-Y., Tseng, Y.-H., Tsang, D.C.W., Hu, A., Yu, C.-P., 2019. Wetland plant microbial fuel cells for remediation of hexavalent chromium contaminated soils and electricity production. J Hazard Mater 365, 137–145.
[19] Clevenger, T., 1990. Use of sequential extraction to evaluate the heavy metals in mining wastes. Water Air Soil Pollut 50, 241–254.
[20] Degryse, F., Verma, V.K., Smolders, E., 2008. Mobilization of Cu and Zn by root exudates of dicotyledonous plants in resin-buffered solutions and in soil. Plant Soil 306, 69–84.
[21] Xing, Y., He, W., Cai, C., Liu, S., Jiang, Y., Tan, S., et al., 2025. Bacterial activation level determines Cd(II) immobilization efficiency by calcium-phosphate minerals in soil. J Hazard Mater 488, 137341.
[22] Symes, J.L., Kester, D.R., 1984. Thermodynamic stability studies of the basic copper carbonate mineral, malachite. Geochim Et Cosmochim Acta 48, 2219–2229.
[23] De Putter, T., Mees, F., Decrée, S., Dewaele, S., 2010. Malachite, an indicator of major Pliocene Cu remobilization in a karstic environment (Katanga, Democratic Republic of Congo). Ore Geol Rev 38, 90–100.
[24] Luo, X.-S., Xue, Y., Wang, Y.-L., Cang, L., Xu, B., Ding, J., 2015. Source identification and apportionment of heavy metals in urban soil profiles. Chemosphere 127, 152–157.
[25] Bonanno, G., 2011. Trace element accumulation and distribution in the organs of Phragmites australis (common reed) and biomonitoring applications. Ecotoxicol Environ Saf 74, 1057–1064.
[26] Kassambara, A., Mundt, F., 2016. Factoextra: extract and visualize the results of multivariate data analyses. CRAN Contrib Packages.
[27] Marchiol, L., Assolari, S., Sacco, P., Zerbi, G., 2004. Phytoextraction of heavy metals by canola (Brassica napus) and radish (Raphanus sativus) grown on multicontaminated soil. Environ Pollut 132, 21–27.
[28] Antoniadis, V., Golia, E.E., Shaheen, S.M., Rinklebe, J., 2017. Bioavailability and health risk assessment of potentially toxic elements in Thriasio Plain, near Athens, Greece. Environ Geochem Health 39, 319–330.
[29] Subrahmaniam, H.J., Picó, F.X., Bataillon, T., Salomonsen, C.L., Glasius, M., Ehlers, B.K., 2025. Natural variation in root exudate composition in the genetically structured Arabidopsis thaliana in the Iberian Peninsula. N Phytol 245, 1437–1449.
[30] Haldar, S.K., 2017. Chapter 1 - Introduction. In: Haldar, S.K. (Ed.), Platinum-Nickel-Chromium Deposits. Elsevier, pp. 1–35.
[31] Ostellari, P., Tapparelli, M., Bragaggia, G., Sandon, A., Lavagnolo, M.C., Girardi, L., et al., 2025. Hydroxy-carboxylic acids as green and abundant ligands for sustainable recovery of copper from a multimetallic powder: a proof of concept. ChemSusChem 18, e202401389.
[32] Shabani, M., Irannajad, M., Azadmehr, A., 2012. Investigation on leaching of malachite by citric acid. Int J Miner Metall Mater 19, 782–786.
[33] Zhang, X., Dippold, M.A., Kuzyakov, Y., Razavi, B.S., 2019. Spatial pattern of enzyme activities depends on root exudate composition. Soil Biol Biochem 133, 83–93.
[34] Mir, A.R., Pichtel, J., Hayat, S., 2021. Copper: uptake, toxicity and tolerance in plants and management of Cu-contaminated soil. BioMetals 34, 737–759.
[35] Leitenmaier, B., Küpper, H., 2013. Compartmentation and complexation of metals in hyperaccumulator plants. Front Plant Sci 4, 374.
[36] Meier, S., Alvear, M., Borie, F., Aguilera, P., Ginocchio, R., Cornejo, P., 2012. Influence of copper on root exudate patterns in some metallophytes and agricultural plants. Ecotoxicol Environ Saf 75, 8–15.
[37] Parveen, A., Saleem, M.H., Kamran, M., Haider, M.Z., Chen, J.-T., Malik, Z., et al., 2020. Effect of citric acid on growth, ecophysiology, chloroplast ultrastructure, and phytoremediation potential of jute (Corchorus capsularis L.) seedlings exposed to copper stress. Biomolecules 10, 592.
[38] Wang, R.-X., Wang, Z.-H., Sun, Y.-D., Wang, L.-L., Li, M., Liu, Y.-T., et al., 2024. Molecular mechanism of plant response to copper stress: a review. Environ Exp Bot 218, 105590.
[39] Schnepf, A., Leitner, D., Klepsch, S., 2012. Modeling phosphorus uptake by a growing and exuding root system. Vadose Zone J 11 vzj2012.0001.
[40] Vetterlein, D., Doussan, C., 2016. Root age distribution: how does it matter in plant processes? A focus on water uptake. Plant Soil 407, 145–160.
[41] Schamphelaire, L.D., Bossche, L.Vd, Dang, H.S., Höfte, M., Boon, N., Rabaey, K., et al., 2008. Microbial fuel cells generating electricity from rhizodeposits of rice plants. Environ Sci Technol 42, 3053–3058.
[42] Rusyn, I., Fihurka, O., Dyachok, V., 2022. Effect of plants morphological parameters on plant-microbial fuel cell efficiency. Innov Biosyst Bioeng 6 (3-4), 161–168.
[43] Rabaey, K., Verstraete, W., 2005. Microbial fuel cells: novel biotechnology for energy generation. Trends Biotechnol 23, 291–298.
[44] Simeon, I.M., Weig, A., Freitag, R., 2022. Optimization of soil microbial fuel cell for sustainable bio-electricity production: combined effects of electrode material, electrode spacing, and substrate feeding frequency on power generation and microbial community diversity. Biotechnol biofuels Bioprod 15, 124.
[45] Rusyn, I., Medvediev, O., 2024. Stacking and design optimization of novel plant microbial fuel cell based on dwarf indoor decorative and culinary plants as a compact biobattery for a low energy consumption devices. Bioresour Technol Rep 26, 101860.
[46] Colmer, T., 2003. Long-distance transport of gases in plants: a perspective on internal aeration and radial oxygen loss from roots. Plant Cell Environ 26, 17–36.
[47] Reddy, K.R., DeLaune, R.D., Inglett, P.W., 2022. Biogeochemistry of wetlands: science and applications. CRC press.
[48] Logan, B.E., Regan, J.M., 2006. Microbial fuel cells—challenges and applications. Environ Sci Technol 40, 5172–5180.
[49] Ancona, V., Cavone, C., Grenni, P., Gagliardi, G., Cosentini, C., Borello, D., et al., 2024. Plant microbial fuel cells for recovering contaminated environments. Int J Hydrog Energy 72, 1116–1126.
[50] Fukai, T., Ushio-Fukai, M., Kaplan, J.H., 2018. Copper transporters and copper chaperones: roles in cardiovascular physiology and disease. Am J PhysiolCell Physiol 315, C186–C201.
[51] Migocka, M., Malas, K., 2018. Chapter 4 - Plant responses to copper: molecular and regulatory mechanisms of copper uptake, distribution and accumulation in plants.

In: Hossain, M.A., Kamiya, T., Burritt, D.J., Phan Tran, L.-S., Fujiwara, T. (Eds.), Plant Micronutrient Use Efficiency. Academic Press, pp. 71–86.

[52] Li, Y., Kawashima, N., Li, J., Chandra, A.P., Gerson, A.R., 2013. A review of the structure, and fundamental mechanisms and kinetics of the leaching of chalcopyrite. Adv Colloid Interface Sci 197-198, 1–32.

[53] Shu, J., Lei, T., Deng, Y., Chen, M., Zeng, X., Liu, R., 2021. Metal mobility and toxicity of reclaimed copper smelting fly ash and smelting slag. Rsc Adv 11, 6877–6884.